



Numerical investigation of labyrinth-shaft spillway

M. Cihan Aydın¹ · Ali Emre Ulu¹

Received: 5 November 2021 / Accepted: 16 February 2023 / Published online: 6 March 2023
© The Author(s) 2023

Abstract

In the present study, a new type of hybrid spillway termed labyrinth-shaft spillway was introduced to improve the discharge capacity and efficiency of the spillway. An advanced computational fluid dynamics (CFD) technique was used to analyze the performance of the labyrinth-shaft spillway. The hydraulic performance of the new model was investigated for different labyrinth geometries with a verified computational model. The analysis results demonstrated that the discharge capacity of the labyrinth-shaft spillway was better when compared to that of the conventional shaft spillways with the same weir heads. The discharge coefficient that reflects the efficiency of the labyrinth-shaft spillway was also much better when compared to the conventional spillway, while the opposite was observed with relatively small nappe heads. Similarly, the comparison with the findings of previous studies on labyrinth weirs in the literature demonstrated that labyrinth-shaft spillways performed better when compared to the conventional labyrinth weirs in-channel flow conditions, especially with high nappe heads. A new formula was also developed in the present study with regression analysis conducted on the collected data to calculate the discharge coefficients of the labyrinth-shaft spillway for $H/P > 0.2$.

Keywords Labyrinth-shaft spillway · CFD · Hybrid design

Introduction

Shaft spillways (i.e., morning glory, bell-mouth shaft spillways) with a drop shaft are preferred especially in cases where the space is restricted on the body and the side banks of the dams and to avoid undesired vibrations on an arch dam body. They are also an economical solution in terms of recycling of the diversion tunnels that could be nonfunctional after construction. These spillways generally include an annular inlet, vertical shaft and outflow tunnel. When the spillway is drowned for high nappe heads, vortices could form in the mouth of the spillway, leading to an unstable flow. This may cause structural vibrations in the spillway and even in the shaft water backflow. In certain cases, some specific tools such as anti-vortex plates are used to prevent the vortex. However, vortex could also help dissipation of the spillway flow energy in the vertical shaft.

In the past, certain studies attempted to develop various designs to improve the hydraulic capacity of shaft spillways due to inlet limitation in the reservoir. For this, it is a good idea to increase the crest length of the spillway in any way. Some researchers such as Bagheri et al. (2010), Cicero et al. (2011), Loisel et al. (2013), Ackers et al. (2013), Shemshi and Kabiri-Samani (2017), Kashkaki et al. (2019), and Aydın and Ulu (2021) and (2023) applied some innovative crest shapes called, i.e., piano-key, daisy-shape, papaya, siphon spillway to improve discharge capacity of the shaft spillways. They concluded that the enhanced crested shaft spillways generally exhibited significant increase in the discharge performance when compared conventional annular shaft spillways with a constant head. In another study, Fattor and Bacchiega (2009) modified the numbers and location of piles on the crest of a morning glory spillway. They concluded that the implemented modifications showed a substantial improvement in hydraulic performance of the spillway.

Some other researchers studied on the swirling and vortex effects, which play roles on the energy dissipation, air entrainment and discharge efficiency in the vertical shaft of the spillways. Shemshi and Kabiri-Samani (2017) and Liu et al. (2018) proposed new shaft spillways types to generate

✉ Ali Emre Ulu
aliemreulu@gmail.com

M. Cihan Aydın
mcaaydin@gmail.com

¹ Department of Civil Engineering, Bitlis Eren University, Bitlis, Turkey

swirling flow by using piers and circular piano-keys on the annular crest. Their findings demonstrated that the swirling flow strength in the modified spillway was several times lower when compared to that of the conventional spillway. Furthermore, they reported that the structure significantly increased the discharge capacity significantly. Zhao et al. (2006) conducted certain model experiments to determine the performance of a vortex drop structure. They found a good correlation between air entrainment rate and water jet velocity, and a good energy dissipation in the vortex drop structure. Kabiri-Samani and Borghai (2013) employed rectangular anti-vortex plates to reduce vortex intensity and air entrainment in a vertical shaft spillway. The design ensured an increase in water discharge when compared to a similar free-surface vortex with the same water head, while decreasing free-surface vortex strength. Xianqi (2015) proposed a new internal rotational flow shaft spillway for high arch dams. The simple structured design provided not only a stable higher capacity water discharge, but also a high-energy dissipation rate and low construction costs.

As in the other hydraulic structures, conventional method to analyze hydrodynamics of the shaft spillways is to use experimental tests. However, in recent years, the use of computational methods in hydraulic engineering has risen significantly. In some case studies on the subject, Enjilzadeh and Nohani (2016) employed a three-dimensional numeric model to analyze the flow hydrodynamics in a morning glory spillway. They calibrated and validated the numerical model with experimental data. The numerical model findings obtained with FLOW-3D exhibited good fit with the experimental findings. Razavi and Ahmedi (2017) developed a flow model for a morning glory spillway with CFD code to investigate the effects of suspended flow load on discharge performance. Ackers et al. (2013) numerically investigated a piano-key weir instead of the original ogee weir around the rim of the bell-mouth spillway at Black Esk reservoir with a CD model. Sabeti et al. (2019) investigated the hydrodynamic properties of a sectoral (radial) morning glory spillway using numerical and physical models.

In recent decades, the interest in labyrinth weirs have increased due to their discharge performance when compared to other weirs. Falvey (2003) reported the hydraulic and design characteristics of the labyrinth weirs in detail. Crookston et al. (2019) presented a perspective for prototype structures, advancement opportunities and future research requirements in labyrinth and piano-key weir hydraulics in a forum paper. Several other researchers such as Crookston and Tullis (2012a, 2013a, b), Aydın (2012), Aydın and Emiroglu (2013, 2016), Bilhan and Emiroglu (2016) and Bilhan et al. (2018) conducted detailed experimental and numerical studies on labyrinth weirs. Crookston and Tullis (2012b) indicated that these weirs could also improve

storage capacity, especially in large reservoirs. Based on the above-mentioned literature, the main advantages of labyrinth weirs include higher discharge capacity and efficiency when compared to traditional linear weirs, especially with a low nappe head, due to the improved crest length. They also ensure an effective solution for space limitations in linear weir crest positions. Considering the advantages of the both spillways (shaft and labyrinth), a new modified spillway design was introduced in the current study. The hydraulic performance of this hybrid spillway design was investigated with computational fluid dynamics (CFD) models.

Numerical method

CFD is an advanced technique that could solve fluid motion equations using the finite volume method for complex viscous flows. The numerical analyses were conducted with the FLOW-3D software, which is widely used worldwide in fluid flow simulations. The Reynolds stress model (RSM) approach is commonly preferred for the description of turbulent flows and solves several transport equations for Reynolds stresses. Two most favorable turbulence models for Reynolds stresses in solving transport equations to determine turbulent kinetic energy (k) and its dissipation (ϵ) include the standard and RNG k - ϵ models. The RNG k - ϵ model employs a statistical technique called renormalization group theory unlike the standard k - ϵ model. Since the RNG k - ϵ model estimates the flow pressure and velocity better when compared to the standard k - ϵ model, especially in complex flows, the model was recommended by Liu et al. (2018). The general form of fluid flow momentum equations could be described by Navier–Stokes equations in three-dimensional Cartesian coordinate as follows:

$$\begin{aligned} \frac{\partial u}{\partial t} + \frac{1}{V_F} \left[uA_x \frac{\partial u}{\partial x} + vA_y \frac{\partial u}{\partial y} + wA_z \frac{\partial u}{\partial z} \right] &= -\frac{1}{\rho} \frac{\partial p}{\partial x} + G_x + f_x \\ \frac{\partial v}{\partial t} + \frac{1}{V_F} \left[uA_x \frac{\partial v}{\partial x} + vA_y \frac{\partial v}{\partial y} + wA_z \frac{\partial v}{\partial z} \right] &= -\frac{1}{\rho} \frac{\partial p}{\partial y} + G_y + f_y \\ \frac{\partial w}{\partial t} + \frac{1}{V_F} \left[uA_x \frac{\partial w}{\partial x} + vA_y \frac{\partial w}{\partial y} + wA_z \frac{\partial w}{\partial z} \right] &= -\frac{1}{\rho} \frac{\partial p}{\partial z} + G_z + f_z \end{aligned} \quad (1)$$

where u , v and w are velocity components in the directions of x , y and z , respectively; V_F is fluid volume fraction opening to the flow; G_x , G_y and G_z are body acceleration components; and f_x , f_y and f_z are viscous acceleration components. The mass continuity equation for incompressible flow (assuming constant density) could be written as follows:

$$\frac{\partial}{\partial x}(uA_x) + \frac{\partial}{\partial y}(vA_y) + \frac{\partial}{\partial z}(wA_z) = 0 \quad (2)$$

Volume of fluid (VOF) method developed by Hirt and Nichols (1981) is a good choice to achieve a clear interface between the fluid phases:

$$\frac{\partial F}{\partial t} + \frac{\partial 1}{V_F} \left[\frac{\partial}{\partial x} (FA_x u) + R \frac{\partial}{\partial y} (FA_y v) + \frac{\partial}{\partial z} (FA_z w) + \varphi \frac{FA_x u}{x} \right] = F_D + F_S \tag{3}$$

Boundary condition, grid and sensitivity analysis

The boundary condition and grid structures of the numerical model are illustrated in Fig. 1a and b, respectively. In Fig. 1a, S is the symmetry, and P represents the pressure inlet boundary conditions in which water depth and pressure can be defined. Hexahedral structured mesh structures were applied to solution domain with three mesh blocks which are mesh block-1, mesh block-2 (conform mesh) and mesh block-3 (for the vertical shaft) as shown in Fig. 1b. The mesh blocks 2 and 3 are finer than the mesh block-1 to better capture the flow in the spillway. On the solid surface, no-slip wall function was selected.

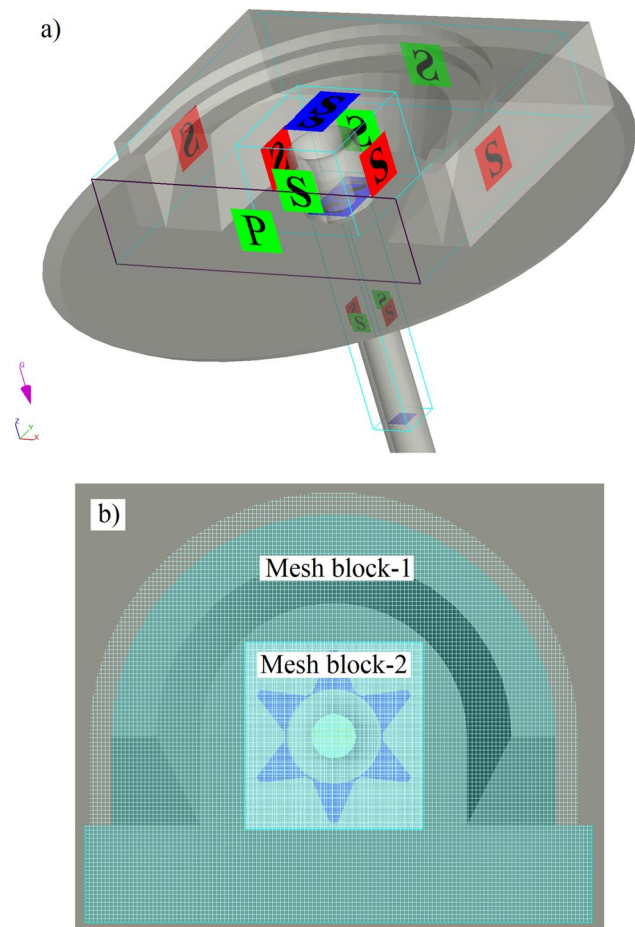


Fig. 1 Numerical model definitions: **a** Boundary condition **b** Mesh structures

In order to reveal mesh sensitivity on numerical solutions, the Grid Convergence Index (GCI) based on the American Society of Mechanical Engineering (ASME) was imple-

mented for three different mesh sizes with the grid refinement factor (*r*) of 1.30 (Celik et al. 2008). The apparent order (*p*) was calculated by following equation for a constant grid refinement factor.

$$p = \frac{1}{\ln r_{21}} \left| \ln \left| \frac{\epsilon_{32}}{\epsilon_{21}} \right| \right| \tag{4}$$

where $\epsilon_{32} = \phi_3 - \phi_2$, $\epsilon_{21} = \phi_2 - \phi_1$, ϕ_k represents the solution on the *k*th grid. The indices 1, 2 and 3 represent the fine, medium and coarse grids, respectively. The extrapolated values are calculated from:

$$\phi_{ext}^{21} = \frac{(r_{21}^p \phi_1 - \phi_2)}{(r_{21}^p - 1)} \tag{5}$$

GCI are calculated for the fine grid solution as follows:

$$GCI_{fine}^{21} = \frac{1.25 \left| \frac{\phi_1 - \phi_2}{\phi_1} \right|}{r_{21}^p - 1} \tag{6}$$

The three sets of grids applied as 682,259, 1,494,566 and 3,261,203 hexahedral cells as coarse, medium and fine mesh, respectively. The global average order of accuracy p_{ave} is 6.41 considered in GCI calculations. The velocity

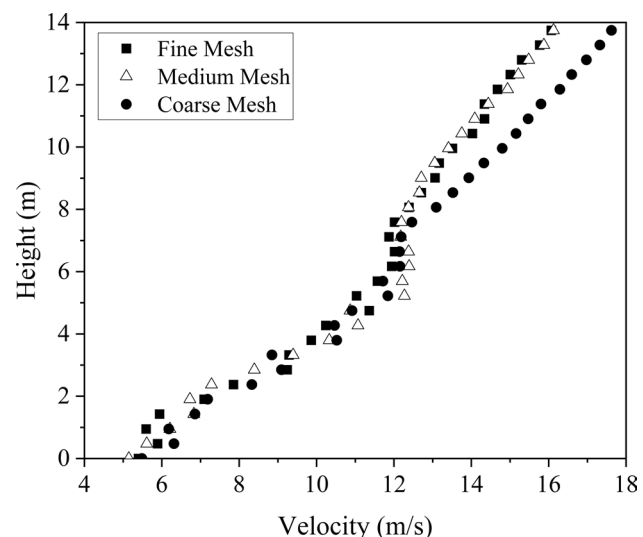


Fig. 2 Mesh sensitivity on velocity of flow in spillway shaft (in which the height of 14 m indicates the crest height)

distributions near the inner surface of the shaft along the height for three different mesh sizes are plotted in Fig. 2. These plots show that the selected mesh sizes have slight effect on the solutions, with a distinct difference for the coarse mesh above 8-m height. In order to make the solutions more sensitive, fine mesh structure was used in the numerical solutions. The maximum GCI_{fine} was estimated as 4.3% for fine mesh solution. This value of the error corresponds to a maximum uncertainty in velocity of about ± 0.24 m/s, and the average relative error is 3.9%, which indicate a good accuracy with respect to the grid sensitivity. In addition, the iterative convergence was achieved with at least three orders of magnitude decrease in the normalized residuals for numerical accuracy.

Calibration with the physical model

In the present study, initially, some physical model data (DSI 2017) for the Kale Dam spillway constructed on Seyhan River in Türkiye were used as a benchmark model to verify and calibrate the numerical model. The sketch of Kale Dam spillway with the prototype dimensions is illustrated in Fig. 3. The scale of the physical model based on the Froude number similarity was selected as 1:20.83 considering laboratory conditions. The diameter of the shaft bell-mouth varied between 11.00 and 5.00 m. Different nappe heads (H) were considered on the crest (between 0.54 m and 2.18) that corresponded the discharges between 26.66 m³/s and 230.12 m³/s based on the stage-discharge rate in the spillway (DSI 2017).

The discharge of a conventional weir could be generally written with the following equation:

$$Q = \frac{2}{3} C_d L \sqrt{2g} H^{\frac{3}{2}} \tag{7}$$

where C_d is the discharge coefficient, L is the crest length, g is the gravitational acceleration, and H is the crest flow head (weir head). This equation could also be used in shaft and labyrinth spillways to calculate the crest length L based

on the planar crest shape. Some researchers such as Tullis et al. (1995) defined the discharge of the labyrinth weirs by considering total upstream head (H_o) as similar to the conventional weir discharge equation. When the approaching flow velocity is very low, the weir head H could be considered equal to the total upstream head H_o as in Eq. (4).

To verify the numerical model, the numerical model results for the conventional shaft spillway were compared to the experimental findings. The 3D numerical model for the conventional shaft spillway based on the prototype dimensions of the benchmark model are presented in Fig. 4. Some illustrations of the experimental (DSI 2017) and the numerical models are presented in Fig. 5. Similar representations in both figures demonstrated that the numerical model was reflected physically. Water discharge and the discharge coefficient, which were the key parameters in the present study and obtained with both experimental and numerical models, are compared in Fig. 6. The findings presented in Fig. 6a demonstrated that there was a reasonable agreement between the two methods. The mean percentage error (MPE) for the numerical and the experimental findings was 9.8% based on the discharge coefficients. The weir discharge curves for both methods are plotted comparatively in Fig. 6b. The comparison also indicated a good agreement between the numerical and experimental models. For the small weir head, the relative error of discharge coefficient was slightly higher than that of the higher heads. This may be due to the effects of

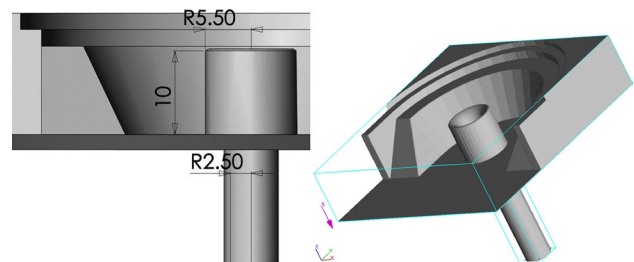
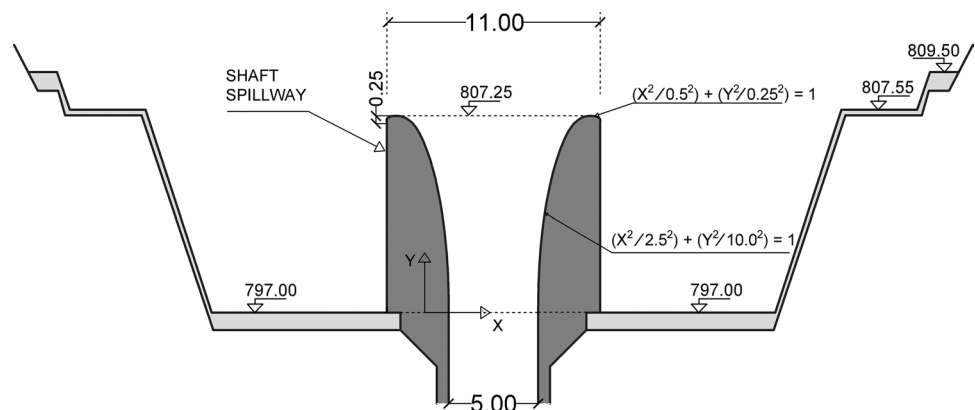


Fig. 4 Numerical model geometry of conventional shaft spillway

Fig. 3 Real dimensions of the physical model in the original project (Dimensions were taken from (DSI 2017))



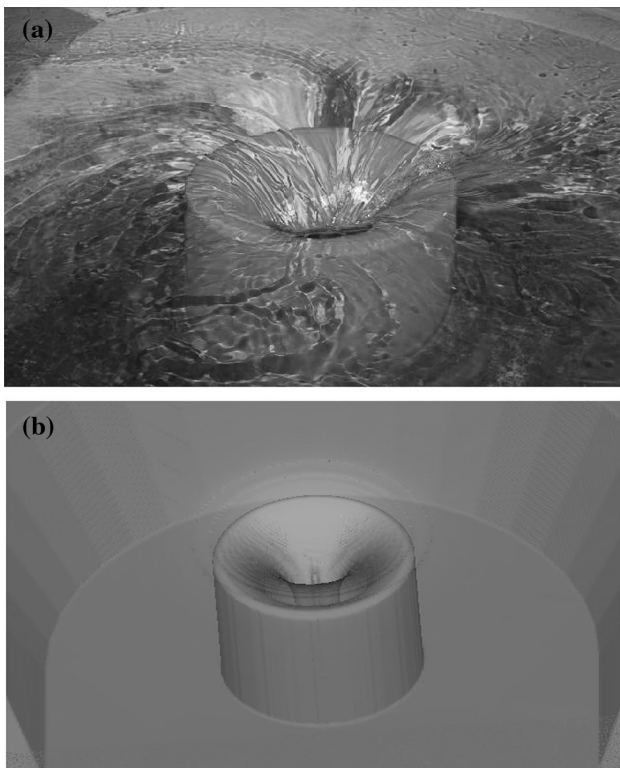


Fig. 5 Models of conventional shaft spillway: **a** experimental (DSI 2017) models, **b** Numerical model runs

scale (i.e., surface tension and viscous effects) on the physical model and the discretization errors in the numerical solutions for low weir heads. Based on these findings, it could be suggested that the numerical model findings were reasonably reliable within the given margin of error, which was approximately lower than 10%. Certain other statistics between the experimental and the numerical flow rates included a 0.197 mean absolute error and a 0.186 root-mean-square error (RMSE).

Analysis of the labyrinth-shaft spillway

Previous studies indicated that the labyrinth crested weirs ensured a higher discharge performance when compared to linear crest weirs for a given channel width. Thus, labyrinth weirs have been widely used to control free overflows in several water structures. To improve the discharge performance, a new hybrid spillway design was developed with a combination of the advantages of the labyrinth and shaft spillway designs. The crest length, which corresponds to cycle apex angle (α), is the most effective factor on labyrinth weir discharge capacity. Therefore, three sharp-crested labyrinth-shaft spillway models with the different apex angles of 30° , 22.5° and 15° were considered as shown in Fig. 7. These designs were analyzed with the above-mentioned

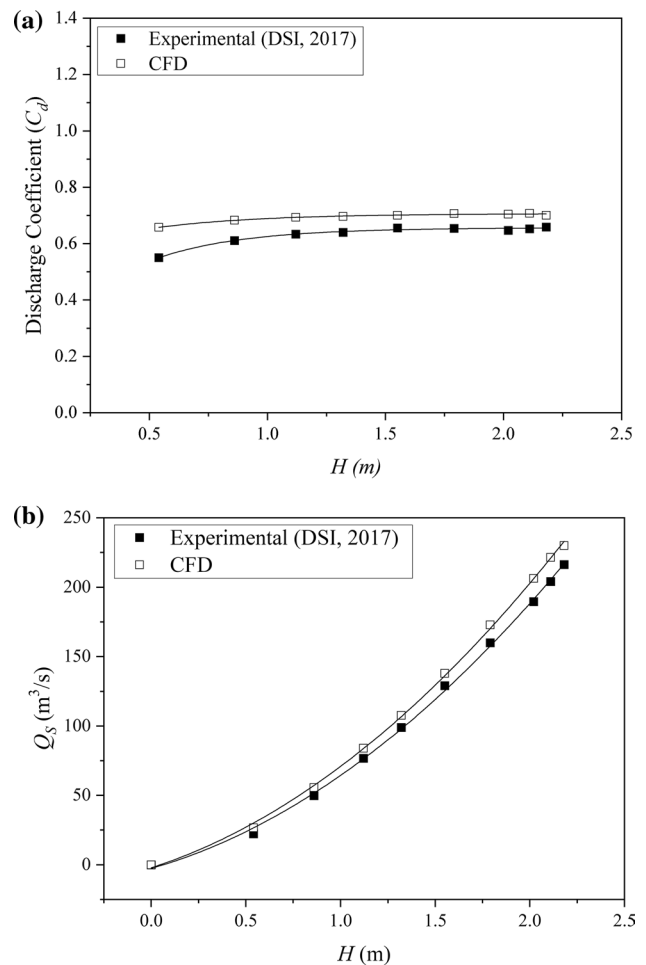
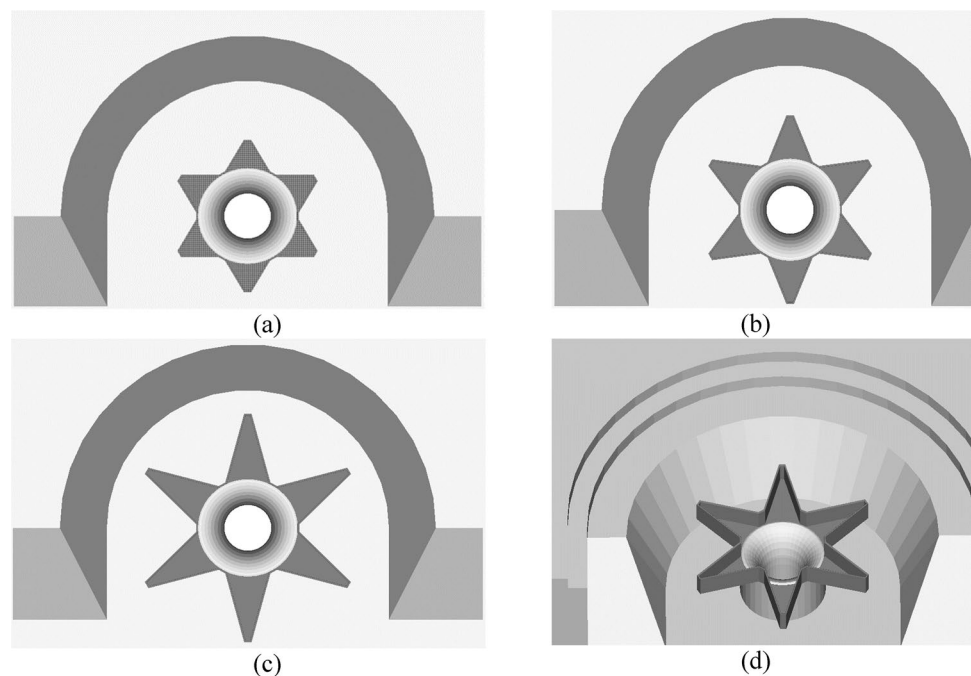


Fig. 6 Comparison of physical and numerical model results: **a** Discharge coefficients versus relative weir head, **b** Head-discharge relationships

computational technique for different weir heads. Certain illustrations obtained with CFD analyses are presented in Fig. 8 for different apex angles and weir heads. As seen in the figure, the weir overflow was free dropping for the small weir head ($H/P=0.18$), and the approaching flow velocity around the labyrinth weir was very low. At higher weir heads, i.e., $H/P=0.52$, the flow was still free overflow; however, the approaching flow velocity around the weir was not significant on the water surface. The effect of the approaching flow on the water surface increases with the decreasing apex angle (that is, increasing weir crest length) and increasing weir head. At the highest nappe head ($H/P=0.73$), the spillway flow is submerged or drowned at the shaft inlet. The drowning effect is further enhanced by the increase in the nappe head and the crest length. Figure 8i shows that the weir overflow is almost completely submerged for $\alpha=15^\circ$, $H/P=0.73$. This means that although the labyrinth crest length increases the flow capacity, this capacity is limited by the shaft capacity.

Fig. 7 Design of labyrinth-shaft spillways with different apex angles: **a** $\alpha = 30^\circ$, **b** $\alpha = 22.5^\circ$, **c** $\alpha = 15^\circ$, **d** 3D view



Results and discussion

The labyrinth-shaft spillway values obtained with the numerical model are presented in Table 1. The weir overflow discharges for different weir heads were compared based on different labyrinth apex angles. As seen in the table, the weir discharge capacity increased with the height of the nappe head and the decrease in the apex angle that corresponded to the increase in weir crest length. However, it could be also observed in the last two columns of Table 1 that the discharge was limited to approximately 350 m³/s due to the shaft capacity. While the weir flow was free dropping in the apex angle of 30° for all nappe heads, the weir flow began drowning after a nappe head of 2.02 m and 1.79 m and an apex angle of 22.5° and 15°, respectively. Thus, the labyrinth-shaft weir drowned unlike conventional linear weirs after a certain nappe head due to the limited capacity of the vertical shaft.

To determine the discharge efficiency of the labyrinth-shaft spillway, Taylor's (1968) equation adopted to the labyrinth weir could be rewritten as follows:

$$\left\{ \frac{Q_L}{Q_S}, C_d \right\} = f \left(\frac{H}{P}, \frac{L}{L_s}, \tan \alpha \right) \quad (8)$$

where Q_L is the labyrinth-shaft weir discharge, Q_S is the discharge of the bell-mouth weir (conventional shaft spillway) with the same diameter. L is the labyrinth weir crest length, and L_s is the shaft spillway crest length (bell-mouth perimeter). The geometric properties of the labyrinth-shaft weir include the apex angle that also corresponds to weir

crest length, bell-mouth diameter (or bell-mouth perpendicular), and the weir height P . Based on Eq. (8), Fig. 9a is plotted to demonstrate the effects of the relative weir head (H/P) on the dimensionless discharge rate (Q_L/Q_S) for different labyrinth apex angles. As seen in the graph, there was a significant correlation between the relative nappe head and the discharge rate, and the relative discharge rate decreased with the increase in the relative nappe head. Otherwise, it was observed that the decrease in the apex angle that corresponds to an increase in crest length significantly improved the dimensionless discharge rate. The discharge rate converged to critical values, which is approximately 1.5 at the relative nappe head of about 0.75. This critical value can be considered as a capacity factor for the labyrinth-shaft spillway.

Discharge coefficient can be determined depending on the channel width W or the total weir crest length L in-channel condition. Here, to reveal the effects of the labyrinth downstream nappe interaction on the discharge efficiency, the crest length-based approach was used to estimate the discharge coefficient (C_d) using the labyrinth crest length (L) instead of the bell-mouth perimeter, as presented in Eq. (7). The discharge coefficient trends versus the relative weir head for different apex angles and the bell-mouth spillways are plotted in Fig. 9b. As seen in the figure, the discharge coefficients of the labyrinth-shaft spillway decreased nonlinearly with the relative weir head (H/P). This decrease was limited for each shape factor. In addition, for a given relative weir head, the discharge coefficient increased with an increase in the apex angle that indicates a decrease in the crest length of the labyrinth weir. When compared to the conventional

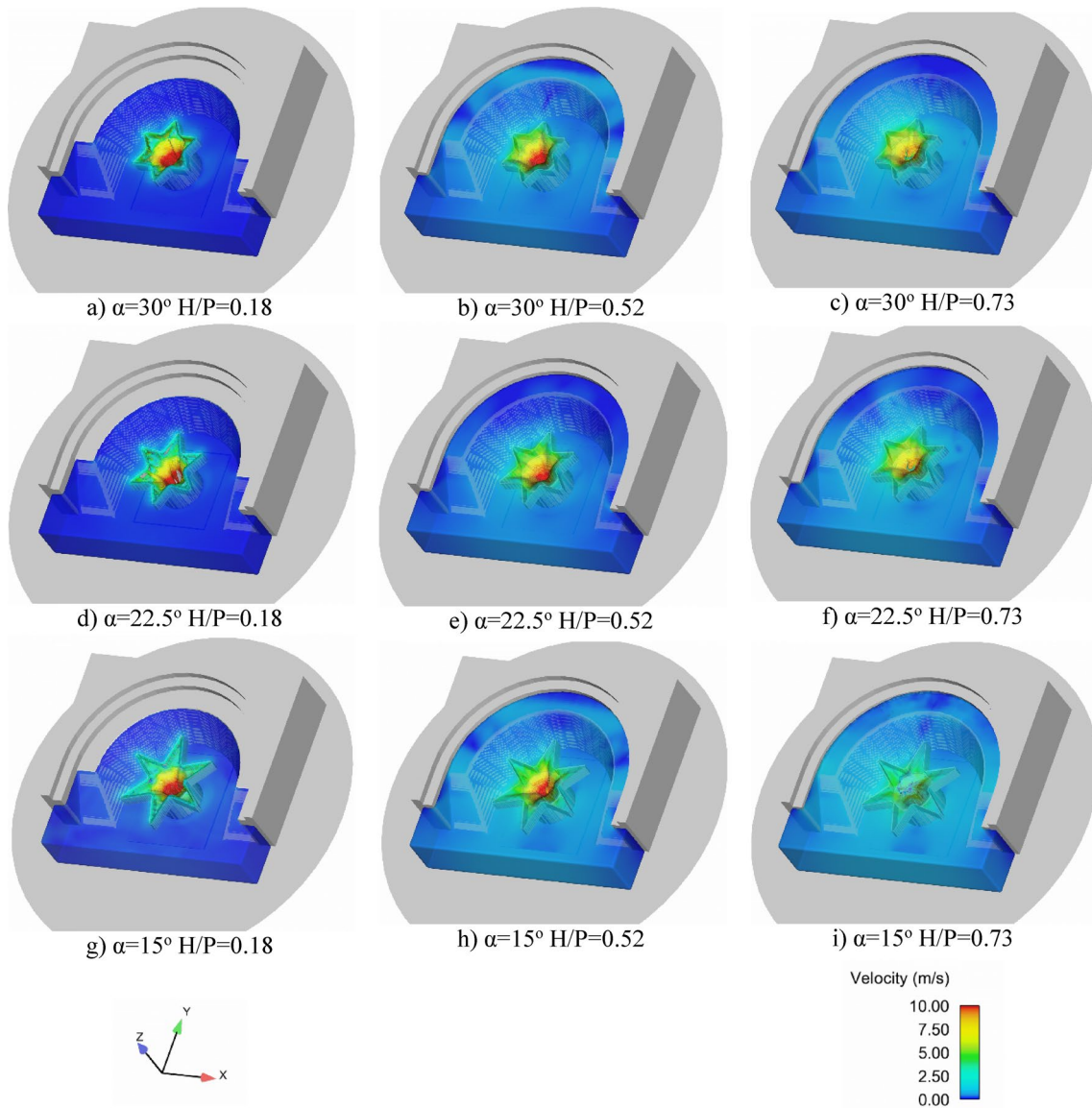


Fig. 8 Simulation views of labyrinth-shaft spillway with different apex angles and nappe heads

Table 1 Discharges values of the labyrinth-shaft weirs for different apex angles

H (m)	H/P (m)	Bell-mouth *Q (m ³ /s)	$\alpha=30^\circ$ *Q ₁ (m ³ /s)	$\alpha=22.5^\circ$ Q ₂ (m ³ /s)	$\alpha=15^\circ$ Q ₃ (m ³ /s)
0.54	0.180	26.66	83.74	88.13	114.14
0.86	0.287	55.60	138.36	137.40	185.88
1.12	0.373	83.92	174.07	183.74	243.8
1.32	0.440	107.81	205.82	223.11	283.49
1.55	0.517	137.99	225.63	273.97	322.79
1.79	0.597	172.86	269.57	297.75	349.91
2.02	0.673	206.41	307.64	339.83	351.05
2.11	0.703	221.49	328.76	353.40	348.76
2.18	0.727	230.12	329.26	350.96	351.47

*These results have been also partly given by Ulu and Aydın (2019)

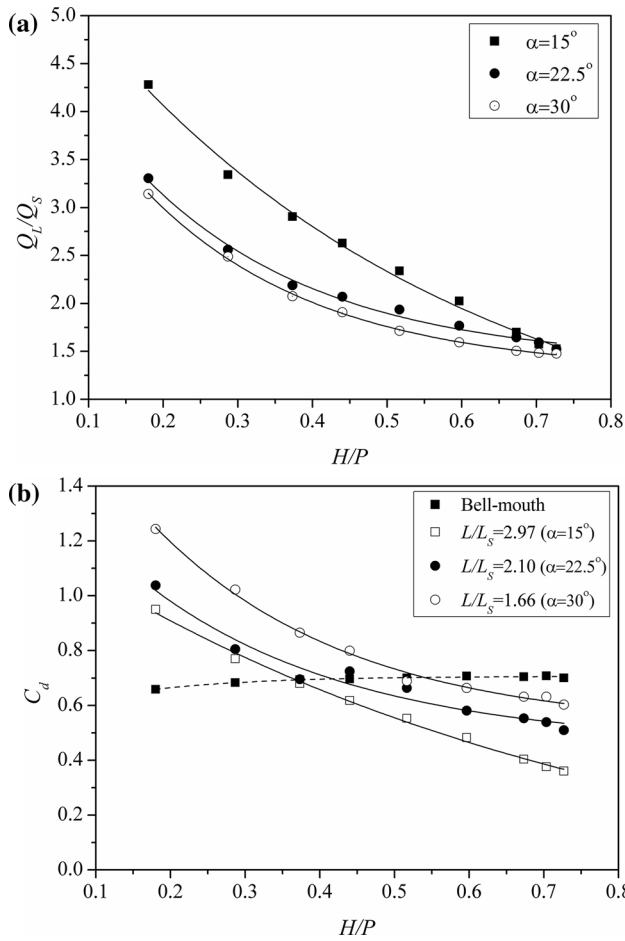


Fig. 9 Effects of relative weir head on: **a** relative discharge rate, **b** discharge coefficients

shaft spillway (bell-mouth), the discharge coefficients of the labyrinth-shaft spillway were higher for low weir heads; however, for higher weir heads (approximately higher than 0.45 of H/P), the discharge efficiency of the labyrinth-shaft spillway was below that of the conventional bell-mouth spillway (Fig. 9b). This could be explained by the nappe interaction just downstream of the labyrinth weir at the high nappe head, thus reducing the effective crest length of the labyrinth weir. Considering the dimensionless parameters of the relative crest length and relative weir head, the following formula was determined to estimate the discharge coefficient of the labyrinth-shaft weirs with $R^2 = 0.97$, as a result of the regression analyses:

$$C_d = 0.91 \left(\frac{L}{L_s} \right)^{-4.06 \frac{H}{P}} + 0.59 \times \exp \left(-0.62 \frac{H}{P} \right) \quad (9)$$

The labyrinth-shaft spillway discharge could be calculated by substituting the discharge coefficient obtained with Eq. (9) in Eq. (7). As seen in Fig. 10, there was a

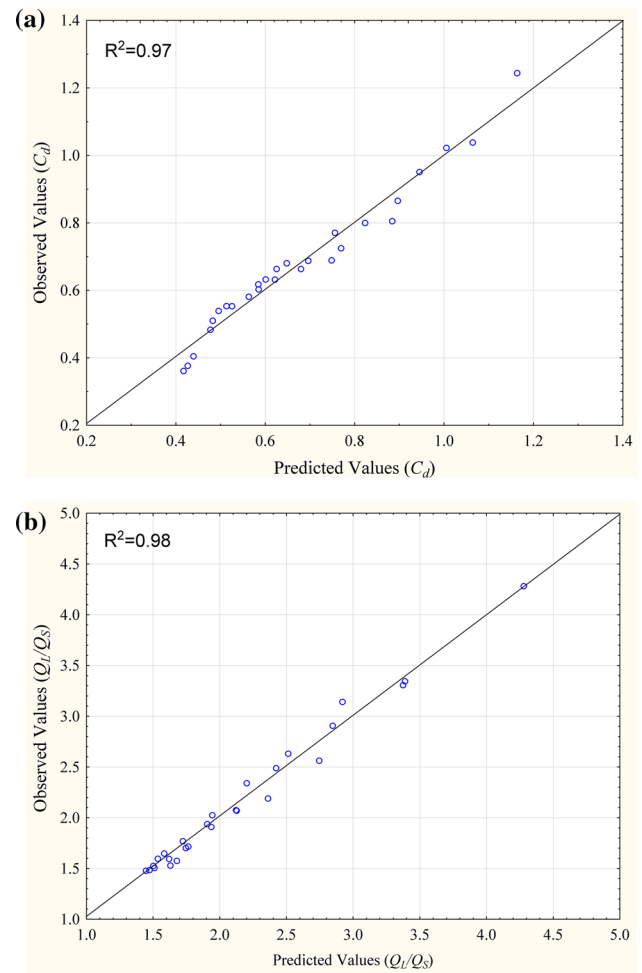


Fig. 10 Observed versus predicted values of: **a** Discharge coefficients (C_d), **b** Relative discharge rate (Q_L/Q_S)

good correlation between the values predicted with Eq. (9) and observed with the discharge coefficients. However, the predicted values deviated slightly from the observed values for the relative discharge rate. It could be suggested that Eq. (9) might be valid only for $H/P > 0.2$. For $H/P < 0.1$, C_d values for the labyrinth-shaft spillway would probably decrease with the decrease in the nappe head, similar to the conventional labyrinth weirs. Since the design discharges for the weir were generally take higher heads into account in practice, the present study focused only on relatively higher weir heads.

To compare the efficiency of the labyrinth-shaft spillway and that of the conventional labyrinth weirs, certain correlations were described in the literature chronologically as follows: Darvas (1971) defined the discharge coefficient of a sharp-crested labyrinth weir depend on the total width of the labyrinth weir (W) and the total head on the weir as follows:

$$C_w = \frac{Q_L}{WH_o^{1.5}} \tag{10}$$

Darvas (1971) plotted a family of curves to determine this coefficient in Eq. (10). It was indicated that the unit of this coefficient was not dimensionless. Megalhaes and Lorena (1989) also proposed certain curves for labyrinth weirs similar to those described by Darvas (1971), except for the ogee crest and dimensional coefficient. This dimensionless coefficient was defined as follows:

$$C_p = \frac{Q_L}{W\sqrt{2g}H_o^{1.5}} \tag{11}$$

The last two equations were given for the total width of the weir W , which were different from C_d , utilized in the present study. The following conversions were used to convert the above terms to dimensionless coefficients based on the developed crest length (L):

$$C_d = \frac{C_p}{\left(\frac{2}{3}\right)\left(\frac{L}{w}\right)} = \frac{C_w}{\left(\frac{2}{3}\right)\left(\frac{L}{w}\right)\sqrt{2g}} \tag{12}$$

Tullis et al. (1995) described the discharge coefficient for triangular labyrinth weirs using certain polynomial curves based on the relative weir head as follows:

$$C_d = A_0 + A_1\left(\frac{H_o}{P}\right) + A_2\left(\frac{H_o}{P}\right)^2 + A_3\left(\frac{H_o}{P}\right)^3 + A_4\left(\frac{H_o}{P}\right)^4 \tag{13}$$

In a similar way, Bilhan and Emiroglu (2016) also defined a fifth-order polynomial equation for trapezoidal labyrinth weirs. In both equations, polynomial coefficients were determined for various apex angles of the labyrinth based on data fitting analysis.

In Fig. 11, the discharge coefficients (C_d) of the labyrinth-shaft spillways, which represent the discharge efficiency, in a reservoir condition were compared with the conventional

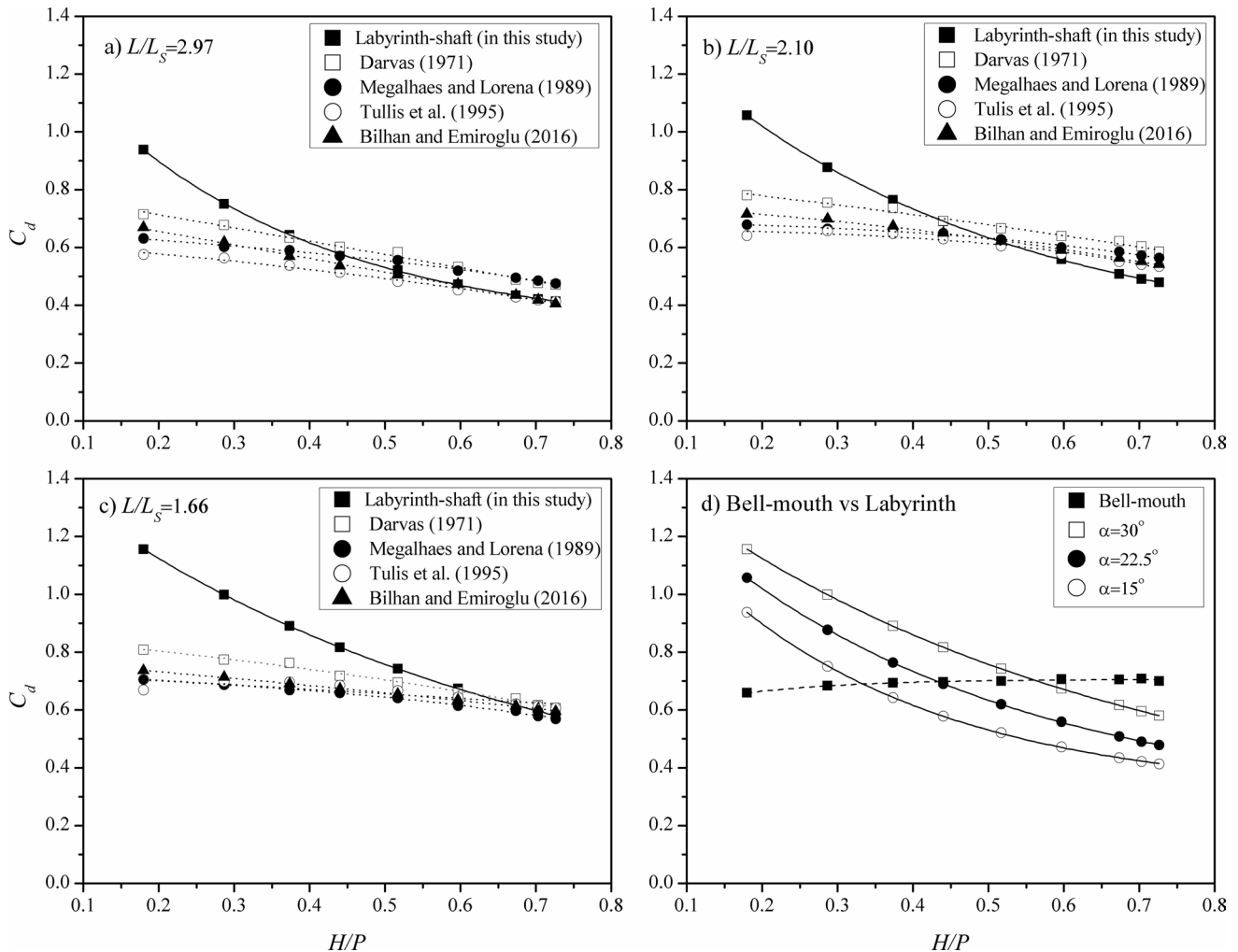


Fig. 11 Comparison of discharge coefficients of labyrinth-shaft weirs with different labyrinth and conventional shaft spillway (bell-mouth)

labyrinth weir findings under in-channel flow conditions based on the relevant literature. As shown in Fig. 11a–c, all findings in the literature for conventional labyrinth weirs were similar. On the other hand, while the efficiency of the labyrinth-shaft spillway was the highest with low weir heads, it decreased and converged to that of the other labyrinth weir types with higher weir heads. With the highest weir heads, the efficiency of the labyrinth-shaft spillways fell below that of the in-channel conventional labyrinth weirs. The decrease with high weir heads was probably due to the local submergence and intense nappe interference as a result of low downstream apex angle values relative to the upstream apex angle of the labyrinths. Crookston and Tullis (2012b) investigated the discharge efficiency of the arced and non-arced labyrinth weirs, and they reported that the arced configuration was the most efficient due to the improved orientation of the labyrinth weir cycles to the approach flow. Crookston and Tullis (2012b) also stated that the C_d reduced with the increase in relative nappe head for $H/P > 0.1$ due to the increase in the local submergence. Local submergence occurs when the discharge carrying capacity exceeds in a labyrinth cycle, leading to a decrease in the efficiency of labyrinth weirs. Therefore, it was determined that the labyrinth weirs were more effective with relatively small weir heads. Since the upstream labyrinth cycle capacities of the labyrinth-shaft weirs are higher than that of the downstream cycles due to their annular axis, the efficiency of the labyrinth-shaft weirs is higher than the conventional weirs for low nappe heads. However, the situation is partly the opposite for high weir heads. On the other hand, the spillway discharge capacity is restricted by the shaft section in the downstream. The results of Eq. (9) were also compared with the efficiency of the conventional shaft (bell-mouth crested) spillway as shown in Fig. 11d. This figure also revealed that the best efficiency was obtained with the widest apex angle; however, the best discharge was obtained with the most acute angle.

An additional formula for calculating the dimensionless discharge rate was also determined with the regression analysis conducted with $R^2 = 0.98$ for $0.2 \leq H/P \leq 0.8$ as follows:

$$\frac{Q_L}{Q_S} = 1.19 \left(\frac{L}{L_S} \right)^{-0.17 \frac{H}{P}} + 1.82 \left(\frac{L}{L_S} \right) \exp \left(-3.04 \frac{H}{P} \right) \quad (14)$$

Using this equation, the discharge of labyrinth-shaft spillways could be calculated based on the discharge of conventional shaft spillway with the same weir inlet diameter. Indlekofer (1978) proposed the following formula for conventional shaft spillway discharge coefficient depend on the ratio of the weir head to bell-mouth radius for $0.2 \leq H/R \leq 0.5$.

$$C_d = 0.515 \left[1 - 0.2 \left(\frac{H}{R} \right) \right] \quad (15)$$

The head-discharge curves for the labyrinth and conventional shaft spillway are plotted comparatively in Fig. 12.

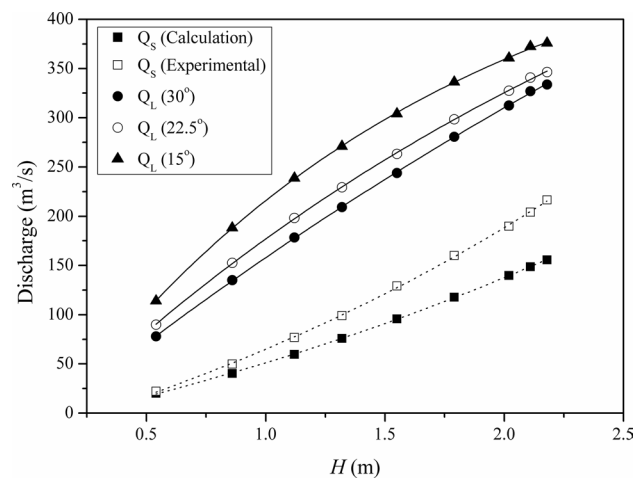


Fig. 12 Comparison of the head-discharge curves of labyrinth-shaft spillway with conventional shaft spillways

The calculated values of Q_s were obtained with Eq. (7) and Eq. (15). As shown in the figure, the calculated values of Q_s were close to the experimental values for the low heads, but not for the high heads in conventional shaft spillways. The gradients of the labyrinth-shaft spillway curves decreased with an increase in the weir, while the curve gradients of the conventional shaft spillway increased with the same effect. In general, it could be suggested that this new hybrid design performed better than conventional designs for all given parameters.

Conclusion

In the present study, a new hybrid spillway design was developed by combining the advantages of the shaft spillway and labyrinth crested weirs. To investigate the hydraulic performance of the spillway, the VOF method with Reynolds-averaged Navier–Stokes and RNG $k-\epsilon$ turbulent models were used in the CFD simulation. The numerical model findings were tested and calibrated with the experimental model findings, and a good agreement was observed between numerical and physical model results with a minor deviation probably due to scale effects in the physical model and convergence errors in the numerical model. The following conclusions could be highlighted based on the study findings:

1. The present study findings demonstrated that the discharge efficiency of the labyrinth-shaft spillway was predominantly dependent on the dimensionless parameters of the weir head (H/P) and labyrinth crest length (L/L_S). Although the discharge efficiency based on the crest length (C_d) decreases with increasing dimensionless crest length (L/L_S), the discharge capacity of the

labyrinth-shaft spillways according to the conventional bell-mouth spillway (Q_L/Q_s) for a certain head increases significantly with the crest length (or decreasing of apex angle). However, the increase in the discharge was limited due to submerged flow conditions in the labyrinths and shaft drowning.

2. The discharge coefficients of the labyrinth-shaft spillway decreased nonlinearly with the relative nappe head (H/P). When compared to the conventional shaft spillway (bell-mouth), the discharge coefficients of the labyrinth-shaft spillway were higher for low nappe head; however, for higher nappe heads (approximately $H/P > 0.45$), the discharge efficiency of labyrinth-shaft spillway was below that of the conventional bell-mouth spillway.
3. Equation (6) determined with the regression analysis presented a good estimate for discharge coefficients for $H/P > 0.2$, which is generally considered in spillway design. The equation presents practical results for hydraulic engineers especially in the initial design of the labyrinth-shaft spillways.
4. The labyrinth cycles in this weir type could also be used as an anti-vortex tool when placed normally or as a vortex generator when placed with asymmetric angles for flow energy dissipation. The effects of the weirs scrutinized in the present study could be investigated further in future studies.

Acknowledgements This study was based on the master's thesis by Ulu (2019). Additionally, we would like to thank to the General Directorate of State Water Works in Türkiye for their valuable contributions.

Funding The author(s) received no specific funding for this work.

Data Availability Some or all data, models, or code that support the findings of this study are available from the corresponding author upon reasonable request.

Declarations

Conflict of interest The authors declare that they have no conflict of interest.

Open Access This article is licensed under a Creative Commons Attribution 4.0 International License, which permits use, sharing, adaptation, distribution and reproduction in any medium or format, as long as you give appropriate credit to the original author(s) and the source, provide a link to the Creative Commons licence, and indicate if changes were made. The images or other third party material in this article are included in the article's Creative Commons licence, unless indicated otherwise in a credit line to the material. If material is not included in the article's Creative Commons licence and your intended use is not permitted by statutory regulation or exceeds the permitted use, you will need to obtain permission directly from the copyright holder. To view a copy of this licence, visit <http://creativecommons.org/licenses/by/4.0/>.

References

- Ackers JC, Bennett FCJ, Scott TA, Karunaratne G (2013) Raising the bellmouth spillway at black esk reservoir using piano key weirs. *Labyrinth and Piano Key*. Taylor & Francis Group, London, pp 235–242
- Aydin MC (2012) CFD simulation of free-surface flow over triangular labyrinth side weir. *Adv Eng Softw* 45(1):159–166. <https://doi.org/10.1016/j.advengsoft.2011.09.006>
- Aydin MC, Emiroglu ME (2013) Determination of capacity of labyrinth side weir by CFD. *Flow Meas Instrum* 29:1–8
- Aydin MC, Emiroglu ME (2016) Numerical analysis of subcritical flow over two-cycle trapezoidal labyrinth side weir. *Flow Meas Instrum* 48:20–28
- Aydin MC, Ulu AE (2021) Aeration performance of high-head siphon-shaft spillways by CFD models. *Appl Water Sci* 11(10):1–12
- Aydin MC, Ulu AE (2023) Developing and testing a novel pressure-controlled hydraulic profile for siphon-shaft spillways. *Flow Meas Instrum* 90:102332
- Bagheri A, Shafai Bajestan M, Moosavi Jahromi H, Kashkooli H, Sedghee H (2010) Hydraulic evaluation of the flow over polyhedral morning glory spillways. *World Appl Sci J* 9(7):712–717
- Bilhan O, Emiroglu ME (2016) Discharge coefficient of sharp-crested trapezoidal labyrinth weirs. *Int J Electron Mech Mech Eng* 16(4):1305–1316
- Bilhan O, Aydin MC, Emiroglu ME, Miller CJ (2018) Experimental and CFD analysis of circular labyrinth weirs. *J Irrig Drain Eng.* [https://doi.org/10.1061/\(ASCE\)IR.1943-4774.0001301](https://doi.org/10.1061/(ASCE)IR.1943-4774.0001301)
- Celik IB, Ghia U, Roache PJ, Freitas CJ (2008) Procedure for estimation and reporting of uncertainty due to discretization in cfd applications. *ASME J Fluids Eng* 130(7):078001
- Cicero GM, Barcouda M, Luck M (2011) Study of a piano-key morning glory to increase the spillway capacity of the Bage dam. *Labyrinth and Piano Key Weir*. Taylor & Francis Group, London, UK
- Crookston BM, Tullis BP (2012) Labyrinth weirs: nappe interference and local submergence. *J Irrig Drain Eng.* [https://doi.org/10.1061/\(ASCE\)IR.1943-4774.0000466](https://doi.org/10.1061/(ASCE)IR.1943-4774.0000466)
- Crookston BM, Tullis BP (2012) Discharge efficiency of reservoir application specific labyrinth weirs. *J Hydraul Eng* 138(6):564–568
- Crookston BM, Tullis BP (2013) Hydraulic design and analysis of labyrinth weirs. I: discharge relationships. *J Irrig Drain Eng.* [https://doi.org/10.1061/\(ASCE\)IR.1943-4774.0000558](https://doi.org/10.1061/(ASCE)IR.1943-4774.0000558)
- Crookston BM, Tullis BP (2013) Hydraulic design and analysis of labyrinth weirs II: nappe aeration, instability, and vibration. *J Irrig Drain Eng.* [https://doi.org/10.1061/\(ASCE\)IR.1943-4774.0000553](https://doi.org/10.1061/(ASCE)IR.1943-4774.0000553)
- Crookston BM, Erpicum S, Tullis BP, Laugier F (2019) Hydraulics of labyrinth and piano key weirs: 100 years of prototype structures, advancements, and future research needs. *J. Hydraul. Eng.* 145(12):02519004
- Darvas LA (1971) Discussion of 'performance and design of labyrinth weirs' by Hay and Taylor. *ASCE, J Hydra Eng* 97(80):1246–1251
- DSI (2017) Physical Model Study of the Kale Dam Spillway (in Turkish). In: Laboratories of General Directorate State Hydraulic Works (DSI), Technical Research and Quality Control Department (Publication No: 1049/415). Ankara, Türkiye.
- Enjilzadeh MR, Nohani E (2016) Numerical modeling of flow field in morning glory spillways and determining rating curve at different flow rates. *Civil Eng J* 2(9):448–457. <https://doi.org/10.1016/j.bjorl.2015.05.003>
- Falvey HT (2003) Hydraulic design of labyrinth weirs. ASCE, Press, American Society of Civil Engineering, 1801 Alexander Bell Drive, Reston, Virginia 20191–4400.

- Fattor CA, Bacchiega JD (2009) Design conditions for morning-glory spillways: Application to Potrerillos Dam spillway. Proceedings of 16th IAHR-APD Congress and 3rd Symposium of IAHR-ISHS, 2124–2128.
- Hirt CW, Nichols BD (1981) Volume of fluid (VOF) method for the dynamics of free boundaries. *J Comput Phys* 39(1):201–225
- Indlekofer H (1978) The computation of crest profiles of cup shaped dam spillways. *Bautechnik* 55(11):368–371
- Kabiri-Samani AR, Borghei SM (2013) Effects of anti-vortex plates on air entrainment by free vortex. *Scientia Iranica A* 20(2):251–258
- Kashkaki Z, Banejad H, Heydari M, Olyaie E (2019) Experimental study of hydraulic flow of circular piano key Inlet in Shaft spillways. *J Rehabil Civil Eng* 7(2):251–257
- Liu ZP, Guo XL, Xia QF, Fu H, Wang T, Dong XL (2018) Experimental and numerical investigation of flow in a newly developed vortex drop shaft spillway. *J Hydraul Eng* 144(5):04018014. [https://doi.org/10.1061/\(ASCE\)HY.1943-7900.0001444](https://doi.org/10.1061/(ASCE)HY.1943-7900.0001444)
- Loisel PE, Duval F, Chanourdie S (2013) Hydraulic scale model of the daisy-shape spillway on the Causse Corrézien dam. Labyrinth and Piano Key Weirs. Taylor & Francis Group, London, UK
- Megalheas AP, Lorena M (1989) Hydraulic design of labyrinth weirs, report No.736. National Laboratory of Civil Engineering, Lisbon, Portugal
- Razavi AR, Ahmedi H (2017) Numerical modelling of flow in morning glory spillways using flow-3D. *Civil Eng J* 3(10):956–964
- Sabeti P, Karami H, Sarkardeh H (2019) Analysis of the impact of effective length of morning glory spillway on its performance (numerical study). *Instrum Mesure Metrologie* 18(2):211–221
- Shemshi R, Kabiri-Samani A (2017) Swirling flow at vertical shaft spillways with circular piano-key inlets. *J Hydraul Res* 55(2):248–258
- Taylor G (1968) The performance of labyrinth weir PhD thesis. University of Nottingham, Nottingham, England
- Tullis JP, Nosratollah A, Waldron D (1995) Design of labyrinth spillways. *ASCE, J Civil Eng* 121(3):247–255
- Ulu AE (2019) Numerical analysis of labyrinth crested shaft spillway. Bitlis Eren University, Institute of Science, Bitlis, Türkiye ((in Turkish))
- Ulu AE, Aydin MC (2019) Shaft spillway with labyrinth crest (a new type spillway), international engineering and natural sciences conference (IENSC 2019), 6–8 November. Dicle University, Diyarbakır, Türkiye
- Xianqi Z (2015) Hydraulic characteristics of rotational flow shaft spillway for high dams. *Int J Heat Technol* 33(1):167–174
- Zhao CH, Zhu DZ, Sun SK, Liu ZP (2006) Experimental study of flow in a vortex drop shaft. *J Hydraul Eng* 132(1):61–68. [https://doi.org/10.1061/\(ASCE\)0733-9429\(2006\)132:1\(61\)](https://doi.org/10.1061/(ASCE)0733-9429(2006)132:1(61))

Publisher's Note Springer Nature remains neutral with regard to jurisdictional claims in published maps and institutional affiliations.